Supplementary Information

Impact of Molecular Charge-Transfer States on Photocurrent Generation in Solid-State Dye-Sensitized Solar Cells Employing Low-Band-Gap Dyes

Sai Santosh Kumar Raavi [1,♦,†], Pablo Docampo[2],[†], Christian Wehrenfennig[2], Marcelo J.P.Alcocer[1,3], Golnaz Sadoughi[2] , Laura L. Herz[2], Henry J. Snaith[2*], Annamaria Petrozza[1]*

1 Center for Nano Science and Technology @PoliMi, Istituto Italiano di Tecnologia, Via Pascoli 70/3, 20133 Milano, Italy

2 Clarendon Laboratory, Department of Physics, University of Oxford, Parks road, Oxford, OX1 3PU, UK

3 Dipartimento di Fisica, Politecnico di Milano, Piazza Leonardo da Vinci 32, 20133 Milano, Italy

[♦] current affiliation: *Division of Physics and Applied Physics, School of Physical and Mathematical Sciences, Nanyang Technological University, 21 Nanyang Link, Singapore 637371*

[†] the authors contributed equally

[*] annamaria.petrozza@iit.it, h.snaith1@physics.ox.ac.uk

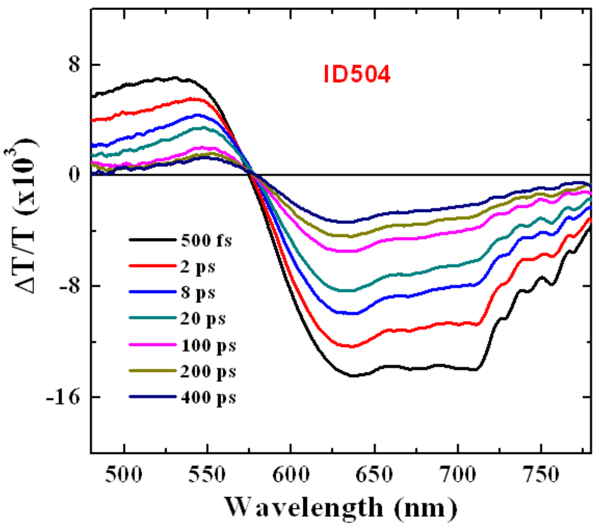
ID504
8
0
-8
-16
ΔT/T (x10^3)
500 fs
2 ps
8 ps
20 ps
100 ps
200 ps
400 ps
500
550
600
650
700
750
Wavelength (nm)

a)

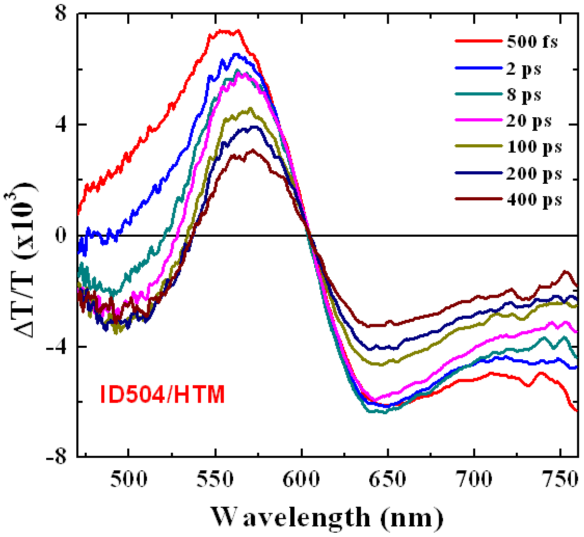
500 fs
2 ps
8 ps
20 ps
100 ps
200 ps
400 ps
8
4
0
-4
-8
ΔT/T (x10^3)
ID504/HTM
500
550
600
650
700
750
Wavelength (nm)

b)

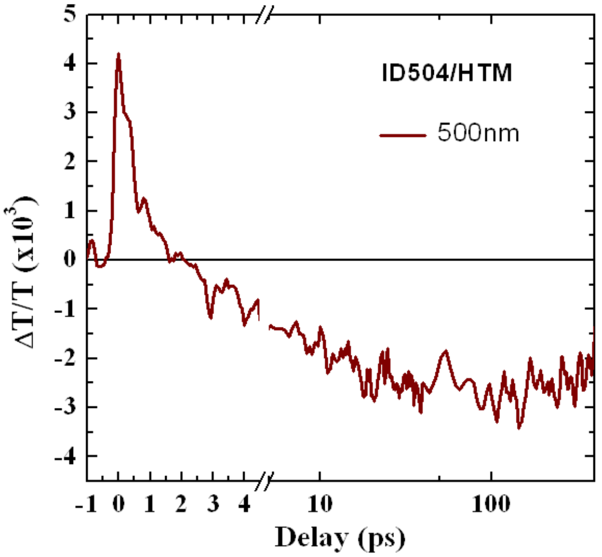
ID504/HTM
500nm
5
4
3
2
1
0
-1
-2
-3
-4
ΔT/T (x10^3)
-1
0
1
2
3
4
10
100
Delay (ps)

c)

Figure S1: a) fs-transient absorption (TA) spectra of ID504 adsorbed on Al_2O_3 upon excitation at 500nm. The positive band ($\Delta T/T>0$) at wavelengths < 570nm is assigned to the ground state photobleaching (PB). The negative band ($\Delta T/T<0$) at wavelengths > 570nm is assigned to the photoinduced absorption (PA) of the singlet excited state ($S_1 \rightarrow S_n$) as no charge generation is expected when the molecule is adsorbed on the high band gap oxide. Thus the spectra evolution over time follows the singlet excited state relaxation to the ground state which may involve also intra-chain electron transfer prior to recombination (note different dynamics in the broad PB band). b) fs-TA spectra of ID504 adsorbed on Al_2O_3 in contact with Spiro-OmeTAd (HTM). The PA band at wavelengths < 550nm and peaking at 500nm is assigned to the absorption of holes in the HTM upon hole transfer from the photo-excited dye. c) Dynamics probed at 500nm from ID504 adsorbed on Al_2O_3 in contact with Spiro-OmeTAd (HTM). It follows the hole transfer from the dye to the HTM.

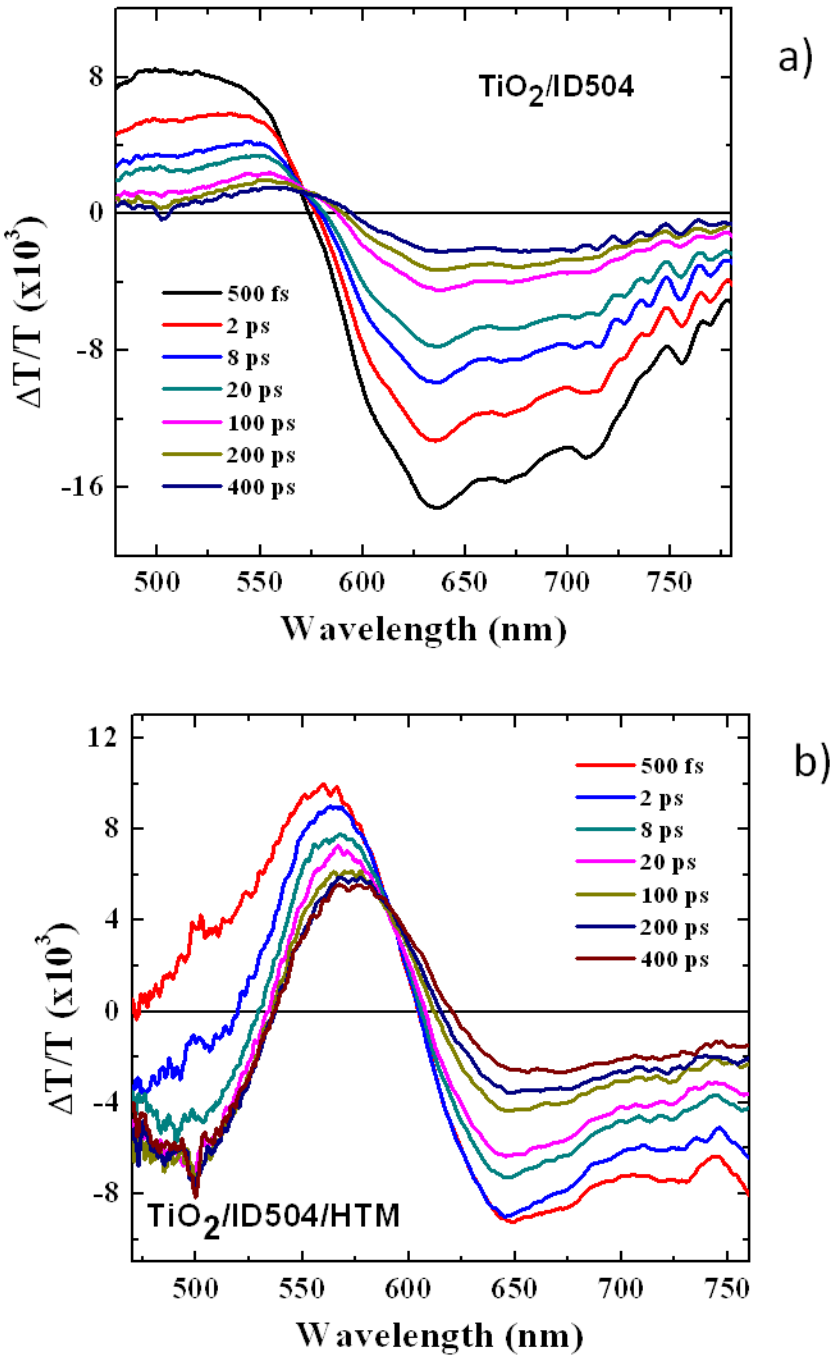

Figure S2: a) fs-transient absorption (TA) spectra of ID504 adsorbed on TiO$_2$ upon excitation at 500nm. The positive band (ΔT/T>0) at wavelengths < 570nm is assigned to the photobleaching (PB). The PB band shift over time denoting multiple processes taking places, i.e. relaxation of the singlet excited state over time and electron transfer to the TiO$_2$. Therefore the PA at longer wavelength is a convolution of different PA bands related to singlet excited states absorption

($S_1 \rightarrow S_n$) and absorption of the oxidized dye. b) fs-TA spectra of ID504 adsorbed on TiO_2 in contact with Spiro-OmeTAd (HTM). The PA band at wavelengths < 550nm and peaking at 500nm is assigned to the absorption of holes in the HTM upon hole transfer from the photo-excited dye.

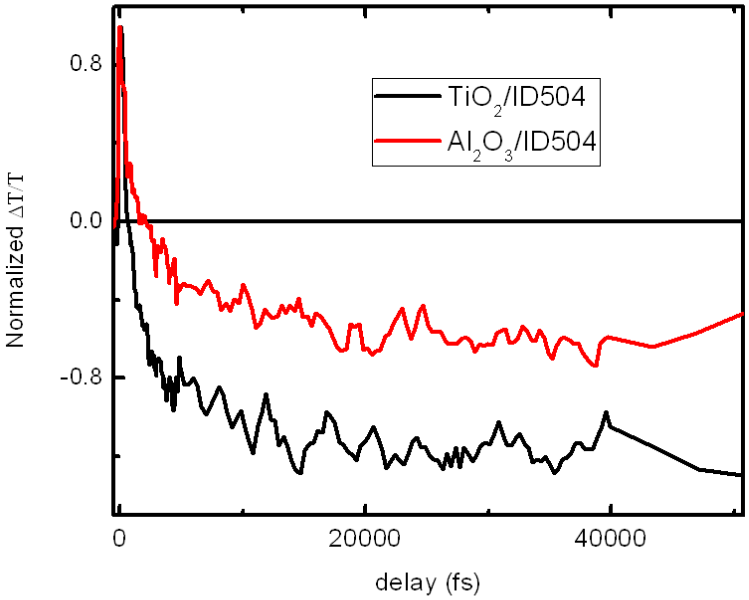

Figure S3: Dynamics probed at 500nm from ID504 adsorbed on Al_2O_3 and on TiO_2 in contact with Spiro-OmeTAd (HTM). They follow the hole transfer from the dye to the HTM when the dye is in contact with a high band gap and an electron –accepting oxide. They reveal a more efficient hole transfer when the oxide does not represent a barrier to electron injection.

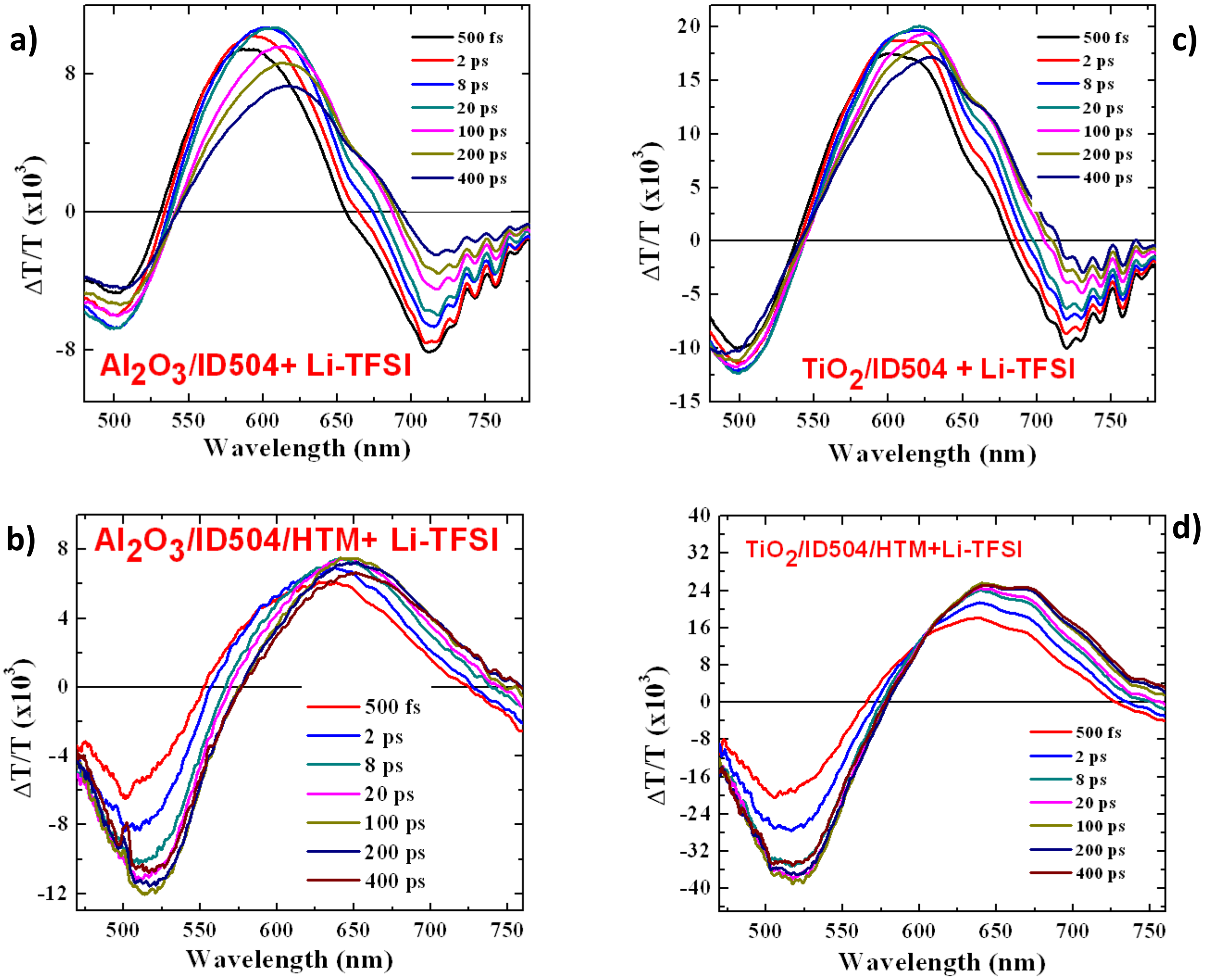

S4: fs-transient absorption (TA) spectra of ID504 adsorbed on Al_2O_3 with and without spiro-OmeTAD (a) and b)) and on TiO_2 with and without spiro-OmeTAD (c) and d)). All samples present Li-TFSI. The spectra show an evident spectral congestion due to the overlapping of different features, i.e. electro-absorption (see Cappel et all, J. AM. CHEM. SOC. 2010, 132, 9096–9101 and Cappel at all, J. Phys. Chem. C 2011, 115, 4345–4358), localized and CT exciton photobleaching, and photo-induced absorption bands. Excitation at 500nm.

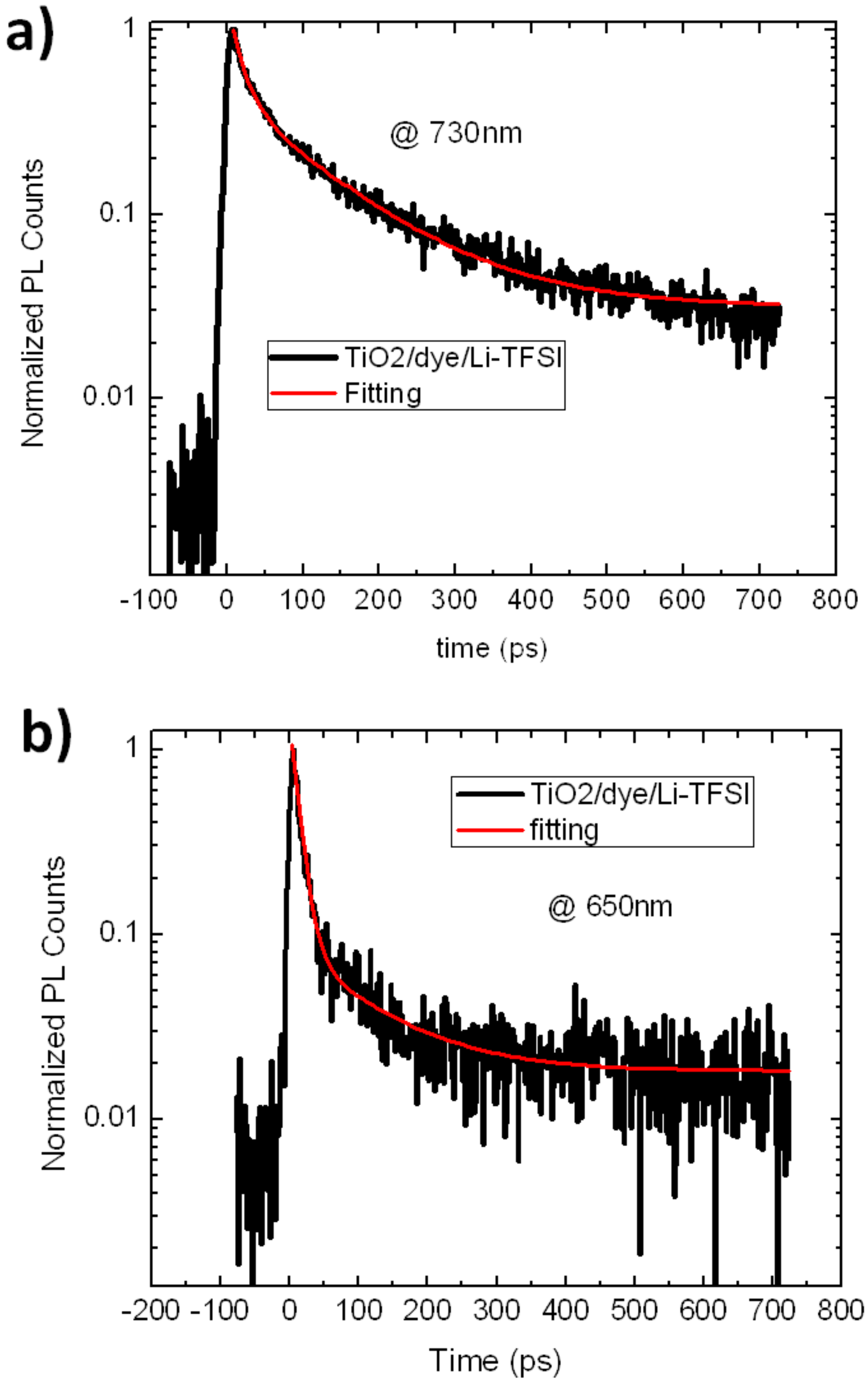
a)
@ 730nm
TiO2/dye/Li-TFSI
Fitting
Normalized PL Counts
1
0.1
0.01
-100
0
100
200
300
400
500
600
700
800
time (ps)
b)
TiO2/dye/Li-TFSI
fitting
@ 650nm
Normalized PL Counts
1
0.1
0.01
-200
-100
0
100
200
300
400
500
600
700
800
Time (ps)

Sigure S5

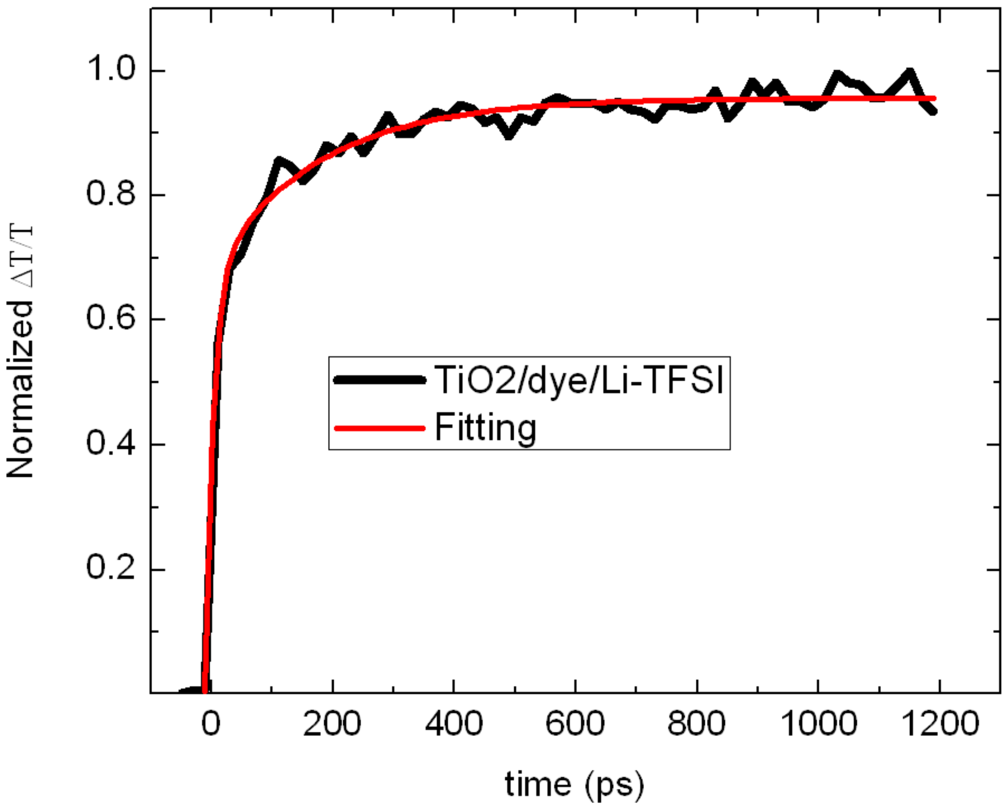

Figure S6

In Figure S5.a the PL decay taken in the low energy emission region (730nm) from sensitized TiO2 mesoporous films in presence of Li-TFSI salts is shown and fitted by a bi-exponential function. Two characteristic lifetimes are found, $\tau_1 \sim 15$ ps and $\tau_2 \sim 120$ ps. On the other hand, the PL decay probed at 650nm, Figure S5.b, is dominated only by one fast decay (faster than 15ps). In Figure S6 we report the THz dynamic from the same sample. It can also be fitted by a bi-exponential function with a first fast rising time of about 13 ps and long tail of 170ps. It is clear that while the PL decay probed in the high energy range may probe both the electron transfer from the dye to the TiO2 and the intra-chain charge transfer on the push-pull system, the PL decay probed in the low energy range follow quite well the electron injection dynamic into the TiO2 probed by THz spectroscopy. This confirms that the low energy state in the dye is the critical/limiting factor in the electron transfer mechanism at the dye/metal oxide interface.

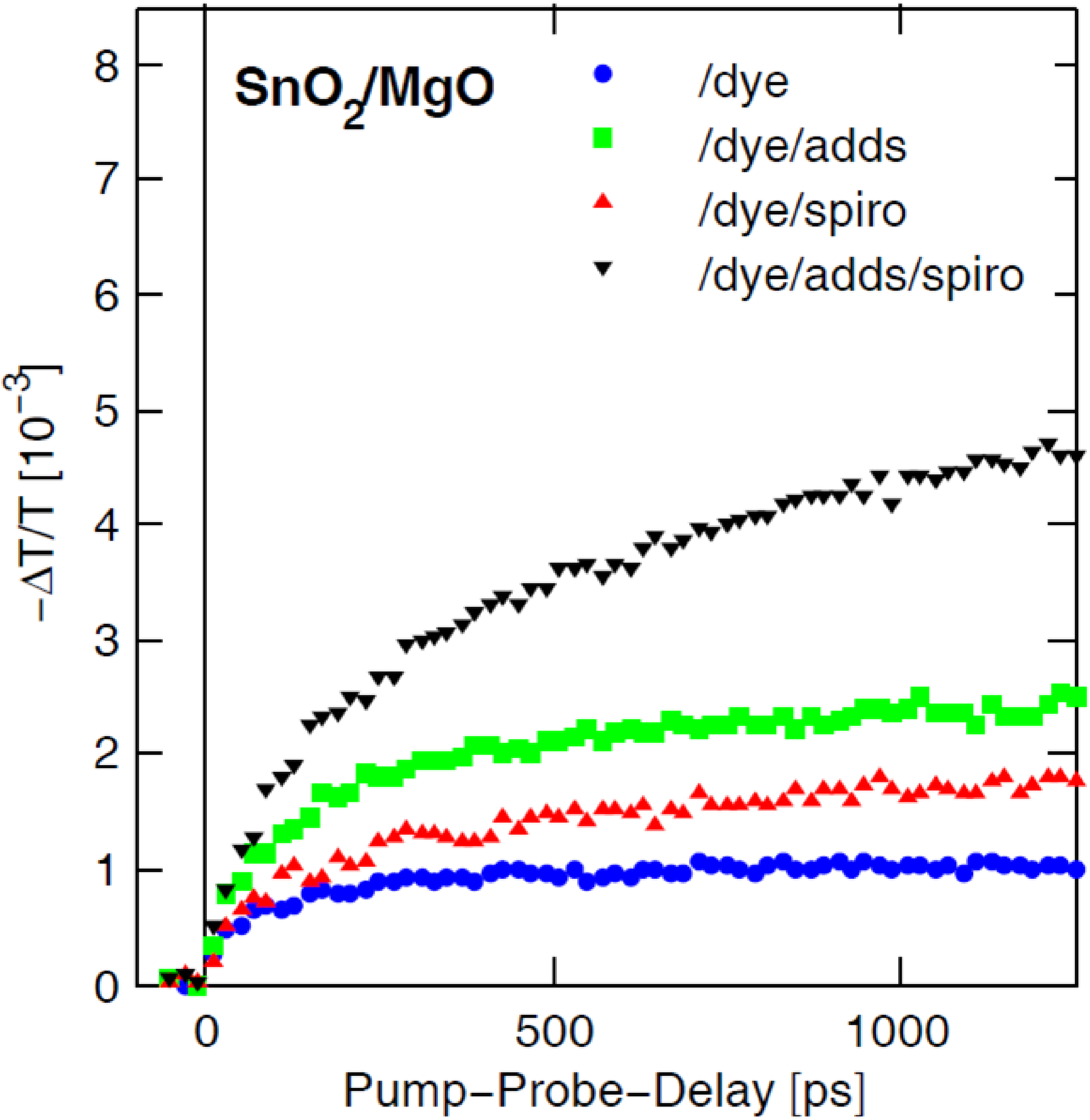

Figure S7: THz dynamics have been measured from samples of SnO2 coated by a thin layer of MgO (S7.a). Though the charge injection is clearly slowed down upon the coating, it must be noted that the dynamics are not affected by the Li-TFSI treatment. Therefore we assume that the slow charge injection is not due to an energy barrier related to the energy levels alignment at the interface, but probably to a different coupling of the dye/MgO density of state. The absence of an actual barrier for electron transfer, as in the TiO2 case, changes the scenario and makes the charge-transfer state again a good precursor for full charge separation, together probably to a reductive quenching. This is well confirmed if we look at the absolute intensity of the THz dynamics in Figures S7 from samples with SnO2/MgO photoanode and we compare to those from TiO2 photoanodes, Fig 3 (note that care was taken in order to maintain the same excitation fluence for each sample in order to consistently compare their signal intensity)

Methods

Transient Absorption: In a typical pump-probe experiment, the system under study is photoexcited by a short pump pulse and its subsequent dynamical evolution is detected by measuring the transmission changes ΔT of a delayed probe pulse as a function of pump-probe delay τ and probe wavelength λ. The signal is given by the differential transmission ΔT/T = [(Tpump on-Tpump off)/Tpump off]. The pump probe set-up is driven by 1 kHz repetition rate pulse train at λ= 780 nm centre wavelength with 150 fs duration produced by a regeneratively amplified mode-locked Ti:Sapphire laser (Clark-MXR Model CPA-1). A fraction of this beam is used to pump an optical parametric amplifier (OPA) capable of delivering tunable pulses in the visible (500 – 700 nm) with ≈10 nm bandwidth and 70-100 fs duration. Another small fraction of the Ti: sapphire amplified output is focused into a 1-mm-thick sapphire plate to generate a stable single-filament white-light supercontinuum which serves as a probe pulse. A short-pass filter with 760-nm cutoff wavelength is used to filter out the residual 800 nm pump light thus limiting our probing window to the (450-760 nm) spectral region. The pump and probe beams are spatially and temporally overlapped on the sample, controlling the time delay by a motorized slit. The minimum detectable signal is $\Delta T/T \sim 10^{-4}$. The system has a ~150 fs temporal resolution. Details of the experimental set-up can be found elsewhere [4]. The pump beam energy density used in the experiment is kept deliberately low (pump fluence= 10 $\mu J/cm^2$) to minimize bimolecular effects. All the measurements were taken with the samples in a vacuum chamber, to prevent any influence from oxygen or sample degradation.